

Article

# Extract Derived from *Cedrus atlantica* Acts as an Antitumor Agent on Hepatocellular Carcinoma Growth In Vitro and In Vivo

Xiao-Fan Huang <sup>1,2</sup>, Kai-Fu Chang <sup>1,2</sup>, Shan-Chih Lee <sup>3,4</sup>, Gwo-Tarng Sheu <sup>1</sup>, Chia-Yu Li <sup>5</sup>, Jun-Cheng Weng <sup>6</sup>, Chih-Yen Hsiao <sup>7,8,\*</sup> and Nu-Man Tsai <sup>2,9,\*</sup>

- <sup>1</sup> Institute of Medicine, Chung Shan Medical University, Taichung 40201, Taiwan; s9870509@gmail.com (X.-F.H.); kfchang1015@gmail.com (K.-F.C.); gtsheu@csmu.edu.tw (G.-T.S.)
  - <sup>2</sup> Department of Medical Laboratory and Biotechnology, Chung Shan Medical University, Taichung 40201, Taiwan
  - <sup>3</sup> Department of Medical Imaging and Radiological Sciences, Chung Shan Medical University, Taichung 40201, Taiwan; sclee@csmu.edu.tw
  - <sup>4</sup> Department of Medical Imaging, Chung Shan Medical University Hospital, Taichung 40201, Taiwan
  - <sup>5</sup> Department of Life and Death, Nanhua University, Chiayi 62249, Taiwan; joyce@nhu.edu.tw
  - <sup>6</sup> Department of Medical Imaging and Radiological Sciences, Chang Gung University, Taoyuan 33303, Taiwan; jcweng@gmail.com
  - <sup>7</sup> Division of Nephrology, Department of Internal Medicine, Ditmanson Medical Foundation Chia-Yi Christian Hospital, Chiayi 60002, Taiwan
  - <sup>8</sup> Department of Hospital and Health Care Administration, Chia Nan University of Pharmacy and Science, Tainan 71710, Taiwan
  - <sup>9</sup> Clinical Laboratory, Chung Shan Medical University Hospital, Taichung 40201, Taiwan
- \* Correspondence: 04504@cych.org.tw (C.-Y.H.); numan@csmu.edu.tw (N.-M.T.); Tel.: +886-4-2473-0022 (ext. 12411) (N.-M.T.); Fax: +886-4-2324-8171 (N.-M.T.)

Academic Editors: Halina Ekiert and Luisa Tesoriere

Received: 31 August 2020; Accepted: 8 October 2020; Published: 10 October 2020



**Abstract:** *Cedrus atlantica* is widely used in herbal medicine. However, the anti-cancer activity of *C. atlantica* extract (CAAt extract) has not been clarified in hepatocellular carcinoma. In the study, we elucidated the anti-hepatoma capacity of CAAt extract on HCC in vitro and in vivo. To explore the anti-hepatoma mechanisms of the CAAt extract in vitro, HCC and normal cells were treated with the CAAt extract, which showed marked inhibitory effects on HCC cells in a dose-dependent manner; in contrast, the CAAt extract treatment was less cytotoxic to normal cells. In addition, our results indicate that the CAAt extract induced apoptosis via caspase-dependent and independent apoptosis pathways. Furthermore, the CAAt extract inhibited HCC tumor cell growth by restraining cell cycle progression, and it reduced the signaling of the AKT, ERK1/2, and p38 pathways. In the xenograft model, the CAAt extract suppressed HCC tumor cell growth and prolonged lifespan by inhibiting PCNA protein expression, repressing part of the VEGF-induced autocrine pathway, and triggering strong expression of cleaved caspase-3, which contributed to cell apoptosis. Moreover, the CAAt extract did not induce any obvious changes in pathological morphology or body weight, suggesting it had no toxicity. CAAt extract exerted anti-tumor effects on HCC in vitro and in vivo. Thus, CAAt extract could be used as a potential anti-cancer therapeutic agent against HCC.

**Keywords:** hepatocellular carcinoma (HCC); *Cedrus atlantica* extract (CAAt extract); cell cycle; apoptosis

## 1. Introduction

Hepatocellular carcinoma (HCC) is the most common type of liver cancer, with an estimated rank of fifth among cancer diagnoses and second among cancer deaths [1]. With the changes in lifestyle

and diet patterns, the incidence and mortality rates of HCC are increasing worldwide [2]. In addition, the average survival rate of patients with HCC is less than three months, owing to the majority of patients being diagnosed in an advanced stage [3,4]. As a result, there are limited therapeutic options for patients, such as transcatheter arterial chemoembolization (TACE), combination chemo-drugs, and targeted therapy [5]. However, these palliative treatments suffer from several problems due to their toxicity and associated side effects [6]. Therefore, it is still urgent to develop a new anti-hepatoma agent for clinical use.

For years, herbs and traditional Chinese medicine have been used in daily life and can be used as foods, flavoring agents, fragrances, or medicines that can alleviate discomfort and improve health. In addition, based on scientific research, various plant extracts have exhibited anti-tumor effects on many types of cancers [7]. Moreover, several studies have reported that plant extracts possess many biological functions, including anti-inflammation and anti-oxidation [8]. Currently, several clinical drugs are extracted from plants, such as etoposide, paclitaxel, irinotecan, and vincristine, which are applied to colon, breast, and lung cancer treatment [9]. Hence, natural plants might be an alternative and viable choice to treat HCC patients owing to their multitarget and coordinated intervention effects.

The genus *Cedrus* contains at least four species: *C. deodara*, *C. libani*, *C. brevifolia*, and *C. atlantica*. Among these, *C. deodara* is widely studied in regard to different biofunctions, such as anti-inflammatory [10], anti-cancer [11–16], anti-oxidant [17], and antimicrobial activities [18,19]. In terms of its anti-cancer activity, it has been shown that *C. deodara* extract has obvious inhibitory effects on tumor growth in various cancers such as leukemia. However, the anti-tumor activity of *C. atlantica* has not been fully explored in vitro or in vivo on liver cancer. *C. atlantica* is an important forest tree species distributed in northern Africa, and its essential oil can be used as a flavoring agent in perfumery and cosmetology. It has been proposed as an antibacterial agent against Gram-positive bacteria [20], and it can alleviate pain by inhalation [21]. Hence, the aim of this study was to investigate the anti-tumor effects and mechanisms of *C. atlantica* extract (CA<sub>t</sub> extract) against HCC in vitro and in vivo.

Our laboratory described the significance of the CA<sub>t</sub> extract on the suppression of HCC tumor growth in vitro and in vivo. Furthermore, we extended our understanding of its anti-cancer mechanisms to the alteration of cell cycle progression, the mediation of cell apoptosis, and the inhibition of cell proliferation. Then, its histopathology was further evaluated. Consequently, our new understanding of the mechanisms of action of the CA<sub>t</sub> extract suggest a potential for CA<sub>t</sub> extract to be developed as an anticancer agent for HCC therapy.

## 2. Results

### 2.1. CA<sub>t</sub> Extract Inhibited the Cell Growth of HCC Cells In Vitro

In exploring the potential inhibitory effects of CA<sub>t</sub> extract against HCC cells, which were treated with a serial dilution of the CA<sub>t</sub> extract for 24, 48, and 72 h, the results revealed that CA<sub>t</sub> extract effectively repressed 50% of HCC cell growth at the concentration of 25 µg/mL (Figure 1A). Among the HCC cell lines assessed, Huh7 cells were the most sensitive, with an 80% decline of viability at 25 µg/mL. In the others, their viability drastically dropped to 20% at a concentration of 50 µg/mL. These results reveal that the viability of HCC cells was reduced in a time- and dose-dependent manner after CA<sub>t</sub> extract treatment. Moreover, the cytotoxicity of the CA<sub>t</sub> extract was examined for normal cells, including BNL CL.2 (mouse normal liver embryonic cells), MDCK (canine normal kidney epithelial cells), and SVEC (mouse normal endothelial cells), and the results show that the CA<sub>t</sub> extract did not apparently affect cell viability below 50 µg/mL at different time points (Figure 1B). Then, as shown in Table 1, the IC<sub>50</sub> values of the CA<sub>t</sub> extract on HepG<sub>2</sub>, Mahlavu, J5, and Huh7 cells were 27.09 ± 1.83 µg/mL, 33.57 ± 2.84 µg/mL, 32.83 ± 4.31 µg/mL, and 6.09 ± 3.28 µg/mL at 24 h. The 50% inhibitory concentrations of the CA<sub>t</sub> extract on normal cells, respectively SVEC, MDCK, and BNL CL.2,

were  $68.03 \pm 4.05 \mu\text{g/mL}$ ,  $69.98 \pm 1.56 \mu\text{g/mL}$ , and  $150.03 \pm 9.57 \mu\text{g/mL}$ . In summary, the CAAt extract effectively inhibited HCC cell growth without markedly being cytotoxic to normal cells.

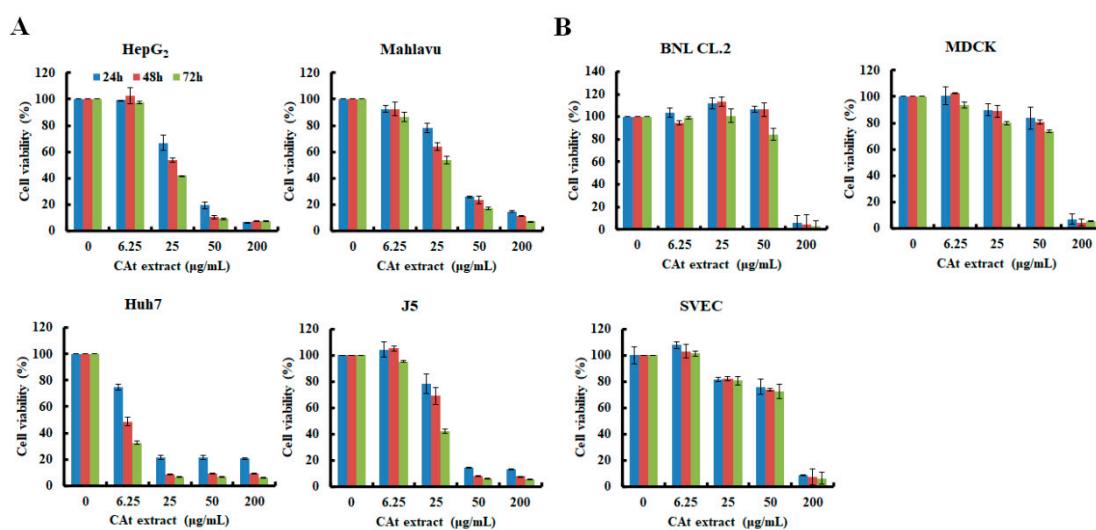


**Figure 1.** Effects of the *Cedrus atlantica* extract (CAAt extract) extract on the growth inhibition of hepatocellular carcinoma (HCC) (A) and normal (B) cells. Cells were cultured in 96-well plates overnight and treated with or without CAAt extract (0–200  $\mu\text{g/mL}$ ) for 24, 48, and 72 h, and evaluated by an MTT assay. Data are expressed as the mean  $\pm$  SD from two independent experiments.

**Table 1.** Anti-proliferative inhibitory activities of the CAAt extract in HCC and normal cells.

Cell Line	Tumor Type	CAAt Extract
<b>Hepatocellular Carcinoma Cell</b>		
HepG <sub>2</sub>	Human HCC cell	$27.09 \pm 1.83$
Mahlavu	Human HCC cell	$33.57 \pm 2.84$
Huh7	Human HCC cell	$6.09 \pm 3.28$
J5	Human HCC cell	$32.83 \pm 4.31$
<b>Normal Cells</b>		
SVEC	Mouse vascular endothelial cell	$68.03 \pm 4.05$
MDCK	Canine epithelial kidney cell	$69.98 \pm 1.56$
BNL CL.2	Mouse liver embryonic cell	$150.03 \pm 9.57$

Note: Values are the mean  $\pm$  SD ( $\mu\text{g/mL}$ ) at 48 h.

## 2.2. CAAt Extract Blocked Cell Cycle Progression at G<sub>0</sub>/G<sub>1</sub> Phase of the HepG<sub>2</sub> and Mahlavu Cells

Former data indicated that CAAt extract showed inhibitory effects on the HepG<sub>2</sub> with wildtype p53 and Mahlavu with mutant p53 (C278L) cells [22,23], and therefore the cell cycle progression was further analyzed. A change of cell cycle was detectable after CAAt extract treatment, and the CAAt extract induced cell cycle arrest at G<sub>0</sub>/G<sub>1</sub> phase in both cell lines (Figure 2A). Moreover, the CAAt extract impeded the cell cycle of HepG<sub>2</sub> cells by increasing the population in G<sub>0</sub>/G<sub>1</sub> phase ( $57.35 \pm 0.86\%$ ,  $61.22 \pm 0.61\%$ ,  $63.13 \pm 0.14\%$ ,  $70.45 \pm 0.62\%$ , and  $81.85 \pm 0.81\%$ ) and reducing S phase ( $18.7 \pm 1.25\%$ ,  $18.75 \pm 0.5\%$ ,  $15.38 \pm 0.10\%$ ,  $16.38 \pm 0.59\%$ , and  $9.33 \pm 0.46\%$ ) as well as G<sub>2</sub>/M phase ( $23.90 \pm 1.77\%$ ,  $20.03 \pm 0.32\%$ ,  $21.49 \pm 0.06\%$ ,  $13.17 \pm 0.14\%$ , and  $8.82 \pm 0.42\%$ ) in a time-dependent manner. Treating HepG<sub>2</sub> cells with different concentrations of the CAAt extract showed that the CAAt extract also induced cell cycle arrest in G<sub>0</sub>/G<sub>1</sub> phase and reduced S phase. The cell cycle distribution of the Mahlavu cells was markedly arrested at G<sub>0</sub>/G<sub>1</sub> phase ( $41.94 \pm 0.78\%$ ,  $54.71 \pm 0.19\%$ ,  $56.42 \pm 1.01\%$ ,  $61.84 \pm 0.66\%$ , and  $58.76 \pm 1.89\%$ ) and there was a significant time-dependent decrease of the S phase ( $24.83 \pm 1.78\%$ ,

21.73 ± 0.64%, 20.6 ± 0.81%, 16.32 ± 0.81%, and 15.44 ± 1.2%) and G<sub>2</sub>/M phase (33.22 ± 1.07%, 23.55 ± 0.45%, 22.94 ± 0.51%, 21.83 ± 0.49%, and 25.79 ± 0.61%) after CA<sub>t</sub> extract treatment (Figure 2B). Additionally, treating Mahlavu cells with different concentrations of CA<sub>t</sub> extract presented a similar trend to accumulate the cell population at G<sub>0</sub>/G<sub>1</sub> phase followed by decreasing both S and G<sub>2</sub>/M phases. These results reveal that the CA<sub>t</sub> extract impeded cell cycle progression at G<sub>0</sub>/G<sub>1</sub> phase in both HepG<sub>2</sub> and Mahlavu cells. Next, the mechanisms of CA<sub>t</sub> extract's regulation of cell cycle in the HepG<sub>2</sub> and Mahlavu cells was examined. As reported in the literature, p53 can induce p21 activation and mediate cyclin/CDK complex degradation (e.g., cdk4 and cyclin D1), resulting in cell cycle arrest. As Figure 2C shows, after CA<sub>t</sub> extract treatment, HepG<sub>2</sub> cells with wild-type p53 dramatically increased p53 and p-p53 (Ser392) expression at 6 h, sustained to 24 h, and diminished at 48 h. Afterward, the level of p21 was also suddenly increased at 6 h and gradually decreased, and the level of cdk4 and cyclin D1 rapidly decreased from 6 h to 48 h. These results reveal that the CA<sub>t</sub> extract rapidly activated p53 and p21, resulting in the downregulation of cdk4 and cyclin D1 in HepG<sub>2</sub> cells. Rb is a tumor suppressor that can alter cell cycle progression to affect cell proliferation. The results indicate that CA<sub>t</sub> extract significantly reduced the level of Rb and p-Rb (Ser24/Thr252) in HepG<sub>2</sub> cells. Further, Mahlavu cells with mutant p53 were observed to have induced p53 and p-p53 (Ser392) expressions, which maintained the protein expression levels from 6 h to 48 h and the level of p21 was abundantly increased at 6 and 12 h, resulting in cdk4 and cyclin D1 expressions being sharply diminished at 6 h after CA<sub>t</sub> extraction treatment. These results reveal that CA<sub>t</sub> extract rapidly increased p21 expression and sustained the increase of activated p53 expression to 48 h to downregulate cdk4 and cyclin D1 quickly. The level of Rb and p-Rb (Ser24/Thr252) was quickly reduced in Mahlavu cells after CA<sub>t</sub> extract, revealing that CA<sub>t</sub> extract repressed Rb and p-Rb expressions were stronger than in HepG<sub>2</sub> cells. Consequently, the CA<sub>t</sub> extract increased p53 and p-p53 (Ser392) and affected downstream protein expressions, including p21, cdk4, and cyclin D1, to affect cell cycle progression. CA<sub>t</sub> extract also moderated Rb and p-Rb (Ser24/Thr252) protein expressions to mediate cell cycle progression in HepG<sub>2</sub> and Mahlavu cells.

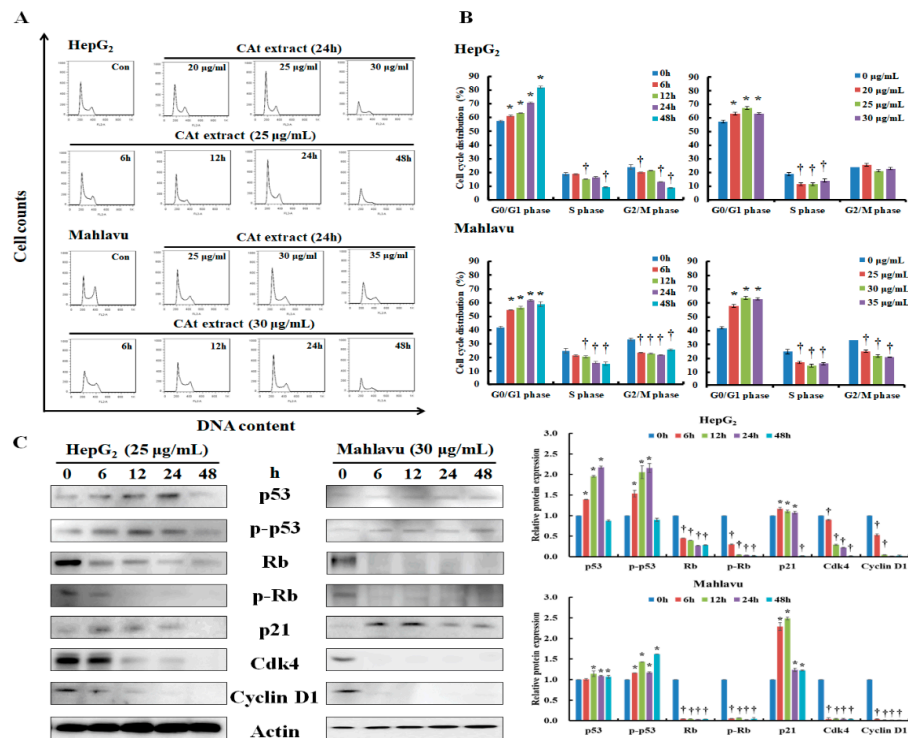


**Figure 2.** Effects of CA extract treatment on the cell cycle distribution and cell cycle regulators expression in HepG<sub>2</sub> and Mahlavu cells. Cells were treated with the indicated CA extract concentrations for 6, 12, 24, and 48 h. After harvesting, the cells were stained with propidium iodide (PI) and analyzed by flow cytometry. Representative diagram of cell cycle progression (A). Representative histograms of cell cycle distribution (B). The protein expression levels of the cell cycle regulators were assessed by Western blot (C). The actin level was used as loading control. \*, †: Significant difference between control and treatment,  $p < 0.05$ .

### 2.3. CA Extract Repressed AKT, ERK, and p38 Protein Expression in HepG<sub>2</sub> and Mahlavu Cells

The biologically relevant signaling pathways of hepatocarcinogenesis involve the AKT, ERK, and p38 pathways [24,25], and thus the expression of these proteins was elucidated by Western blot. After CA extract treatment, AKT protein expression was significantly reduced, and there was also inhibition of the phosphorylation of p-AKT (Ser473/Ser474/Ser472) at 12 h in HepG<sub>2</sub> cells (Figure 3). The protein expression of ERK was decreased at 12 h, and the level of p-ERK (Tyr204) rapidly reduced at 6 h, which continuously declined to 48 h in a time-dependent manner in HepG<sub>2</sub> cells. Further, the level of p-p38 (Tyr182) was decreased by CA extract and showed a similar trend with the inhibition of p-AKT protein expression in HepG<sub>2</sub> cells. In Mahlavu cells, the CA extract significantly reduced AKT protein expression at 24 h and remarkably diminished the level of p-AKT (Ser473/Ser474/Ser472) at 6 h. However, the level of ERK and p-ERK (Tyr204) were not rapidly inhibited by CA extract, and these protein expressions were significantly reduced at 48 h. Next, the level of p38 was reduced at 6 h, lasting to 48 h, and p-38 (Tyr182) was suddenly declined at 6 h in Mahlavu cells. Consequently, the CA extract displayed good inhibitory ability through the AKT/p-AKT, ERK/p-ERK, and p38/p-p38 pathways, which facilitate HCC cell growth.

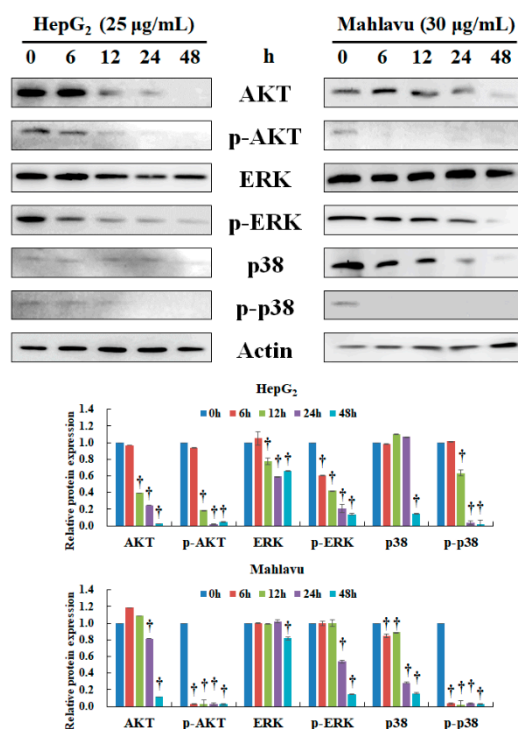


**Figure 3.** Effect of CAT extract treatment on AKT, ERK, and p38 protein expression in HepG<sub>2</sub> and Mahlavu cells. HepG<sub>2</sub> and Mahlavu cells were incubated with CAT extract (25 or 30 µg/mL) for the indicated time points (0, 6, 12, 24, and 48 h) then subjected to Western blotting analysis. The actin level was used as loading control. †: Significant difference between control and treatment,  $p < 0.05$ .

#### 2.4. CAT Extract Induced Cell Apoptosis of HCC Cells through Activation of the Extrinsic and Intrinsic Caspase Cascades

Due to the growth-inhibitory effect of CAT extract on HCC cells, the sub-G<sub>1</sub> phase was further examined to detect whether CAT extract induced cell death. The results reveal that sub-G<sub>1</sub> phase significantly increased to about 60–80% of sub-G<sub>1</sub> phase in both cells in a time- and dose-dependent manner (Figure 4A). Then, the mode and mechanism of CAT extract's induction of apoptotic cell death in HepG<sub>2</sub> and Mahlavu cells were further examined. In the TUNEL assay results, the cell nucleus of the untreated HepG<sub>2</sub> and Mahlavu cells with PI staining were round and flat, and no distinct green fluorescence of TUNEL was observed. However, after treatment with the CAT extract, the nuclei were fragmented into different sizes in most of the cells, and the green fluorescence of TUNEL was strongly visible along with various apoptotic cell morphologies, including anoikis, DNA fragments, chromatin condensation, and apoptotic bodies formation (Figure 4B). Consequently, to investigate the CAT-extract-induced apoptotic mechanisms in the HepG<sub>2</sub> and Mahlavu cells, the apoptosis-associated protein expression levels were evaluated (Figure 4C). The extrinsic apoptosis-related proteins, including FAS, FASL, and procaspase-8, were examined, and the results indicate that the FAS and FASL proteins were upregulated in treated Mahlavu and HepG<sub>2</sub> cells. The downstream pro-caspase-8 protein expression was markedly decreased at 6 h and kept reducing to 48 h, revealing that the extrinsic pathway was activated. The intrinsic apoptotic proteins were also investigated, and the results show that an increment of Bax and a decline of Bcl2 and procaspase-9 were significantly reduced at 48 h in HepG<sub>2</sub> cells, indicating that the intrinsic pathway was turned on. Increasing levels of procaspase-3 and decreasing levels of cleaved caspase-3 were observed at 48 h, suggesting that the caspase cascade was fully activated at 48 h in HepG<sub>2</sub> cells. Besides, the level of AIF (apoptosis-inducing factor) was dramatically increased at 6 h, and that continuously amplified its protein expression in HepG<sub>2</sub> cells. Moreover, the levels of FAS and FASL proteins were sharply increased, followed by a decline of procaspase-8 at 6 h to the activated extrinsic pathway in Mahlavu cells. The intrinsic apoptotic proteins,

including Bax, Bcl2, and procaspase-9, were rapidly affected by the CA<sub>t</sub> extract at 6 h. The levels of Bax and Bcl2 showed a similar trend to what was detected in HepG<sub>2</sub> cells, and the downstream protein procaspase-9 was decreased at 6 h to facilitate activation of the intrinsic pathway in Mahlavu cells. In addition, procaspase-3 protein expression was reduced, and cleaved caspase-3 protein expression was increased in a time-dependent manner in Mahlavu cells. The level of AIF in Mahlavu cells was increased after CA<sub>t</sub> extract treatment, resulting in activation of the caspase-independent pathway. Therefore, the CA<sub>t</sub> extract blocked cell proliferation via the induction of cell apoptosis, including the extrinsic as well as the intrinsic caspase-dependent and independent apoptosis pathways.

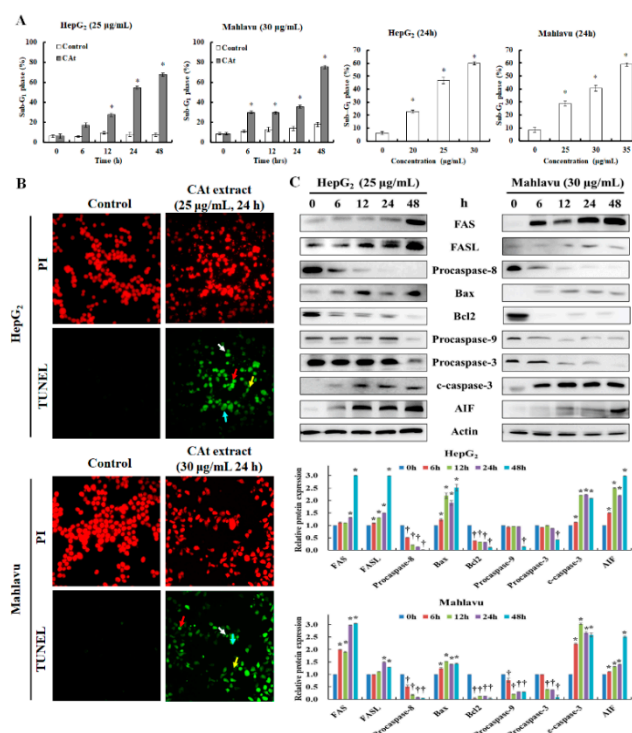


**Figure 4.** Effects of CA<sub>t</sub> extract treatment on apoptosis in HepG<sub>2</sub> and Mahlavu cells. The percentage of sub-G<sub>1</sub> phase which was analyzed by flow cytometry after CA<sub>t</sub> extract treatment with HepG<sub>2</sub> and Mahlavu cells (A). Photograph of TUNEL expression on HepG<sub>2</sub> and Mahlavu cells treated with or without CA<sub>t</sub> extract (25 or 30 µg/mL) for 24 h by fluorescence microscope (B), red arrow: anoikis; blue arrow: chromatin condensation; yellow arrow: DNA fragments; white arrow: apoptotic bodies. Cells treated with CA<sub>t</sub> extract (25 or 30 µg/mL) for 0, 6, 12, 24, and 48 h, and cell lysates were collected for analysis of indicated protein expression. Effects of CA<sub>t</sub>-extract-induced apoptotic protein expression was analyzed by Western blot (C). c-caspase-3: cleaved caspase-3. \*, †: Significant difference between control and treatment,  $p < 0.05$ .

### 2.5. CA<sub>t</sub> Extract Suppressed HCC Xenograft Tumor Growth and Extended Lifespan

To examine the inhibitory potential of the CA<sub>t</sub> extract on HCC tumors, an HCC xenograft model was established. Mice bearing HepG<sub>2</sub> liver cancer xenografts were subcutaneously injected with mineral oil as a vehicle or treated with the CA<sub>t</sub> extract (200 mg/kg, s.c.) every two days. When the tumor volume was greater than 2000 mm<sup>3</sup>, the mice were sacrificed to collect the tumor as well as the organs for follow-up pathological analysis. The data reveal that the CA<sub>t</sub> extract treatment achieved about a 42.3% inhibitory effect at day 39 on the tumor burden of the HCC xenograft compared with the vehicle (Figure 5A; 882.4 ± 62.9 mm<sup>3</sup> versus 2077.2 ± 160.2 mm<sup>3</sup>). The data also demonstrate that the CA<sub>t</sub> extracts prolonged the lifespan from 43 to 51 days compared with the vehicle (Figure 5B). Thus, these data demonstrate that the CA<sub>t</sub> extract has antitumor effects on HCC tumor growth and improves survival outcomes in vivo. Subsequently, to evaluate the CA<sub>t</sub>-extract-induced systematic

toxicity *in vivo*, the body weights of the mice were measured every two days. The results revealed no significant difference between the CAAt extract treatment and vehicle in changes of body weight, suggesting that the CAAt extract might have little toxicity *in vivo* (Figure 5C). In addition, a pathological evaluation of hematoxylin/eosin (H&E)-stained liver and kidney tissues was conducted; there were no obvious changes in tissue morphology (Figure 5D). The results demonstrate that the CAAt extract might show little or no toxicity as assessed by body weight and organ damage.

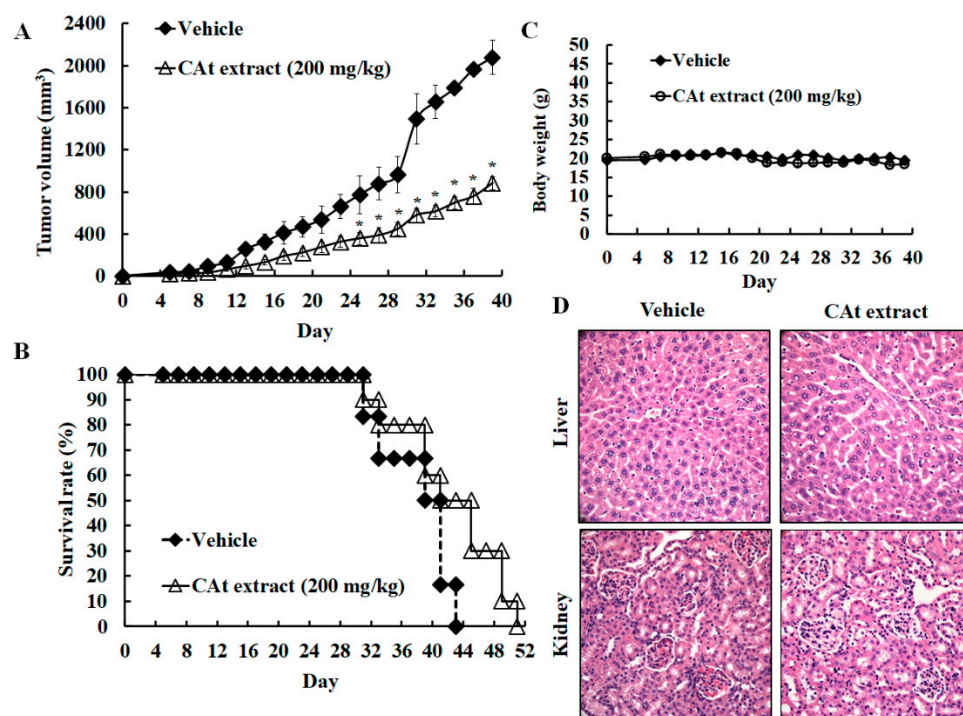


**Figure 5.** The xenograft tumor model of HCC treated with the CAAt extract (200 mg/kg). The tumor suppression (A) and the survival rate (B) of HCC tumor growth after CAAt extract treatment. Evaluation of systemic toxicity of CAAt extract administration on the HCC xenograft. The body weight after CAAt extract treatment (C). The hematoxylin/eosin (H&E) staining of the liver and kidney (D).

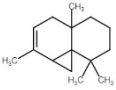
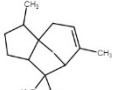
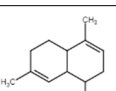
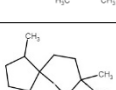
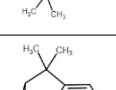
### 2.6. CAAt Extract Exhibited Antihepatoma Capacity via Induction of Apoptosis, Reduction of Cell Proliferation, and a Decline of Metastatic Protein Markers

Next, to further elucidate the mechanisms of the CAAt extract's effects on the HCC xenograft animal model, the CAAt-extract-induced tumor cell damage was observed by H&E staining, and the results reveal that the CAAt extract triggered tumor cell death (Figure 6A). Thus, we looked for evidence of cell apoptosis induced by the CAAt extract. The results show that the protein expression of cleaved caspase-3 was increased and that apoptotic bodies were observed in the tumor tissue (Figure 6B). Moreover, the TUNEL assay revealed that many DNA fragments were observed in many of the hepatoma cells, and the CAAt extract induced a great number of TUNEL-positive cells (Figure 6C). These results reveal that the CAAt extract triggered tumor cell death by inducing cell apoptosis. Then, in order to identify the inhibitory mechanisms of the CAAt extract in HCC xenografts, the protein expression of PCNA, VEGF, VEGFR1, and VEGFR2 were examined by immunohistochemical (IHC) staining. PCNA is expressed during the DNA synthesis phase of the cell cycle. The CAAt extract reduced the expression of the PCNA protein, suggesting that it might possess the ability to affect cell cycle progression in hepatoma cells (Figure 7A). VEGF and its target receptors, VEGFR1 and VEGFR2, were examined in order to investigate the inhibitory effects of autocrine VEGF signaling, which might be affected by the CAAt extract. The results indicate that VEGF, VEGFR1, and VEGFR2 protein expressions were all reduced by the CAAt extract treatment, suggesting the CAAt extract might reduce VEGF autocrine signaling.



Moreover, MMP2 and MMP9 protein expression were tested in order to investigate the anti-metastasis potential of the CA<sub>t</sub> extract, and we found that the CA<sub>t</sub> extract repressed the expression of both MMP2 and MMP9, suggesting that the CA<sub>t</sub> extract might have the potential to suppress HCC invasion by inhibiting MMP2 and MMP9 protein expression (Figure 7B). Taken together, the CA<sub>t</sub> extract might have several anti-HCC effects *in vivo*, with results that are consistent with the data found *in vitro*, including the induction of apoptosis and interruption of cell proliferation. Consequently, we aimed to analyze the effective components in CA<sub>t</sub> extract by GC-MS, and as shown in Table 2, the five major components were thujopsene (43.36%),  $\alpha$ -cedrene (31.67%),  $\alpha$ -cadinene (2.73%), cedrol (1.42%), and isolongipholene (0.52%). Cedrol has reported anti-cancer activity, [26] and might be an effective compound to inhibit HCC cell growth.

**Table 2.** GC-MS analysis of CA<sub>t</sub> extract.

	Compound	Percentage (%)	Chemical Structure	CAS No.	Molecular Weight
1	Thujopsene	43.36%		470-40-6	204.35 g/mol
2	$\alpha$ -Cedrene	31.67%		469-61-4	204.35 g/mol
3	$\alpha$ -Cadinene	2.73%		11044-40-9	204.35 g/mol
4	Cedrol	1.42%		77-53-2	222.37 g/mol
5	Isolongipholene	0.52%		1135-66-6	204.35 g/mol

Note: GC-MS analysis was committed to National Central Taiwan University Office of Research and Development's Center for Advanced Instrumentation (Hsinchu, Taiwan). Components were identified by comparing their mass spectra with those obtained from authentic samples or spectra of the Wiley/NIST libraries.

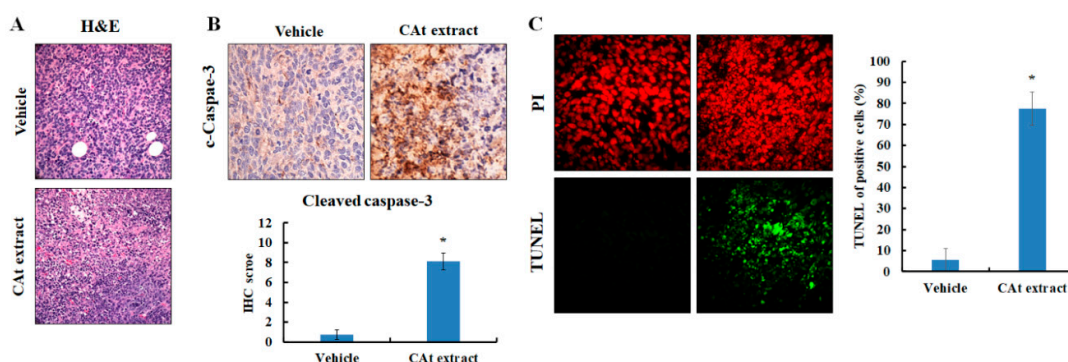


**Figure 6.** CA<sub>t</sub>-extract-induced apoptosis in the HCC xenograft tumor model by H&E, immunohistochemical (IHC), and TUNEL staining. (A) Tissue morphology, evaluated with H&E staining. (B) CA<sub>t</sub>-extract-induced cleaved caspase-3 expression. (C) TUNEL staining for the observation of apoptotic cells. \*: A significant difference between control and treatment,  $p < 0.05$ .

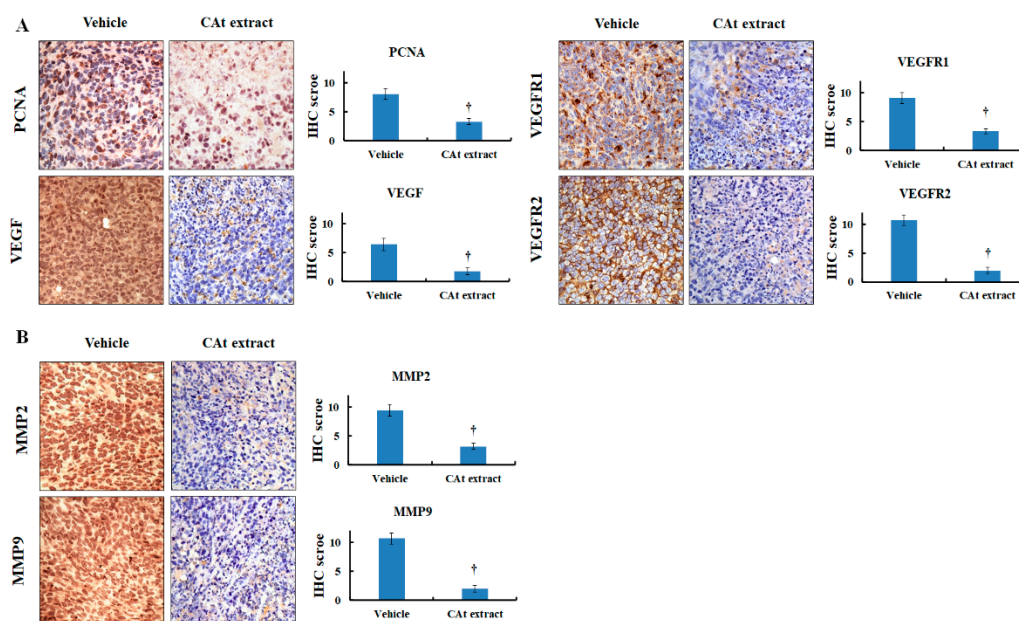


**Figure 7.** CA1-extract-induced inhibitory effect in the HCC xenograft tumor model by IHC staining. Indicated protein expression in HCC tumor tissues was stained by IHC. (A) The level of PCNA, VEGF, VEGFR1, and VEGFR2 protein. (B) The level of MMP2 and MMP9 protein. †: A significant difference between control and treatment,  $p < 0.05$ .

### 3. Discussion

Herbal and plant medicines have been used for centuries worldwide. Furthermore, in recent decades, a significant number of medicinal herbs have been reported to have biofunctional effects in treating chronic liver diseases through eliminating viruses, alleviating fibrogenesis, and suppressing tumorigenesis. As a result, plant extracts can be considered as potential anti-cancer candidates for cancer therapy [9,10]. Here, in the first study to investigate the anti-hepatoma activity of CA1 extract in vitro and in vivo, our results first found that HCC cells were inhibited by CA1 extract; nevertheless, the cytotoxicity of CA1 extract was moderate against normal cells, including liver embryonic cells, kidney epithelial cells, and endothelial cells. The results also indicate that CA1 extract blocked cell cycle progression at  $G_0/G_1$  phase in vitro. In addition, p53 protein prominently increased from 6 to 24 h, and the functional phosphorylated p53 was increased by CA1 extract. The downstream protein, p21, was increased after the increment of p53 and p-p53 protein expression, and cdk4 and cyclin D1 were found to be reduced in a time-dependent fashion. The alteration of the cell-cycle-related protein expression levels contributed to stopping cell cycle progression. Besides, TP53 mutation is associated with a poor prognosis [27]. Our result indicates that CA1 extract exerted an inhibitory effect on both wild-type and mutant p53 HCC cells. Moreover, total Rb and phosphorylated Rb were dramatically decreased within 6 h, which might increase the dissociation rate of E2F and Rb to alleviate cell proliferation. On the other hand, MAPK and AKT/mTOR signaling pathways are essential in controlling cell proliferation, differentiation, and survival, and have been studied to determine the pathogenesis of HCC [24,25]. The AKT/mTOR pathway plays a pivotal role in hepatocarcinogenesis [28,29], and a previous study showed about 53% positive expression of p-AKT protein in HCC tissues and 12% of cirrhotic tissues [30]. Therefore, it is an attractive candidate as an anticancer drug target for HCC treatment. Moreover, ERK can regulate cell cycle progression, apoptosis resistance, cellular motility, and drug resistance. As a result, a repression of ERK was exerted to inhibit the development of HCC and increase cell apoptosis in HCC tumors [31]. We first found that phosphorylated AKT, ERK, and p38 were reduced rapidly within 12 h after CA1 extract treatment, suggesting that CA1 extract has a potential capacity to suppress hepatocarcinogenesis, helping to prevent the development of HCC at an early stage.

Next, we used TUNEL staining to test whether the CA<sub>t</sub> extract induced cell apoptosis, and found that many cells were TUNEL green positive. The details of the mechanism of apoptosis induction were examined. After CA<sub>t</sub> extract treatment, FAS and FASL expression increased at 12–24 h, which might have caused the expression of the procaspase-8 protein to decrease at 12 h dramatically. However, procaspase-8 decreased before FAS and FASL protein increased, which suggests that the CA<sub>t</sub> extract might regulate the extrinsic apoptotic pathway via different mechanisms, which we explored further. CA<sub>t</sub> extract might not directly affect the intrinsic apoptotic pathway, as Bax, Bcl2, and procaspase-9 proteins did not show rapid declines in HepG<sub>2</sub> cells. In the Mahlavu cells, the CA<sub>t</sub> extract rapidly increased Bax protein expression and sharply decreased Bcl2 and procaspase-9 protein expression at 6 h. In the late stage of apoptosis, CA<sub>t</sub> extract strongly and quickly induced cleaved caspase-3 protein expression in both cell lines. These results reveal that CA<sub>t</sub> extract triggered cell apoptosis via extrinsic as well as intrinsic apoptosis pathways. The alteration of AIF protein expression was greatly increased at 12 to 24 h, suggesting that CA<sub>t</sub> extract induced not only the caspase-dependent pathway but also activated the caspase-independent pathway, which contributed to cell apoptosis. Taken together, the results suggest that CA<sub>t</sub> extract suppressed HCC tumor growth via the inhibition of cell cycle progression, induction of cell apoptosis, and suppression of AKT, ERK, and p38 signaling *in vitro*.

In the xenograft model, the results first demonstrate that CA<sub>t</sub> extract exerted a good HCC tumor-suppression ability. As seen by H&E staining, a marked anaphase cell morphology of the HCC tissue was observed. Many of the cell bodies were shrinking and the cell nuclei were fragmenting, resulting in cell death. Similarly, HCC tumor tissue stained for TUNEL revealed that the CA<sub>t</sub> extract induced cell apoptosis, with the formation of apoptotic bodies and DNA fragmentation. In addition, cleaved caspase-3 was strongly expressed, confirming that CA<sub>t</sub> extract induced cell apoptosis of HCC *in vitro*. Former results revealed that CA<sub>t</sub> extract regulated cell-cycle-related proteins to impede cell cycle progression. PCNA is a proliferation marker and can stand for the status of cell cycle. Moreover, HCC cells highly express PCNA, which increases during late G<sub>1</sub> or very early S phases of the cell cycle [32]. As a result, in an *in vivo* study, PCNA was assayed in order to evaluate whether CA<sub>t</sub> extract affected cell cycle progression. CA<sub>t</sub> extract efficiently reduced PCNA protein expression, indicating that it inhibited HCC tumor cell growth, consistent with the results observed *in vitro*. Subsequently, we wondered whether CA<sub>t</sub> extract repressed VEGF/VEGFR-induced autocrine or paracrine proliferation *in vivo*; therefore, VEGF, VEGFR1, and VEGFR2 expressions were examined. In addition, VEGF/VEGFR signaling not only plays a critical role in the angiogenesis of HCC, but also has a vital role in the autocrine progression of HCC [33,34]. Previous studies have reported that VEGFR1 and VEGFR2 are overexpressed in HCC, and high levels of VEGF, VEGFR1, and VEGFR2 indicate a poor prognosis [35,36]. The results indicate that CA<sub>t</sub> extract exerted an inhibitory potential in the suppression of VEGF/VEGFR-induced autocrine or paracrine proliferation by downregulating VEGF, VEGFR1 and VEGFR2 expressions *in vivo*. Hence, these results provide a different and potential inhibitory effect of CA<sub>t</sub> extract by the restriction of the VEGF/VEGFR autocrine growth pathway to suppress HCC tumor growth and improve the prognosis of HCC patients. Additionally, some studies have indicated that the activated PI3K/AKT signaling pathway is correlated with hepatic cancer progression and promotes VEGF/VEGFR1 expression [37–39]. Therefore, the results might also suggest that CA<sub>t</sub> extract not only inhibited the activated AKT expression of upstream protein *in vitro* but also repressed VEGF, VEGFR1, and VEGFR2 expressions *in vivo* to suppress HCC tumor cell growth. Furthermore, CA<sub>t</sub> extract reduced MMP2 and MMP9 protein expression, which play essential roles in the invasion, revealing that CA<sub>t</sub> extract might possess anti-invasion activity *in vivo*. Hence, CA<sub>t</sub> extract was observed to have multiple functions in this study: growth inhibition, reduction of autocrine signaling, induction of apoptosis, and suppression of metastasis. To further find the antihepatoma compound in CA<sub>t</sub> extract, our results reveal that the cedrol might be one of the effective anticancer ingredients in CA<sub>t</sub> extract due to its anticancer activity in non-small-cell lung cancer [26], and others might need to conduct further study to explore the anticancer activity in future.

During hepatocarcinogenesis, the liver function is damaged due to virus attack, alcohol abuse, or the accumulation of fatty acids. Therefore, liver toxicity is an important criterion for clinicians to evaluate the feasibility of treating HCC patients. We thus evaluated the changes of body weights and the pathological alterations of liver and kidney tissue after treatment with CA<sub>t</sub> extract. The results reveal that the CA<sub>t</sub> extract had almost no effect on body weight during the whole course of treatment. The liver tissue showed healthy liver cells with the filling of the cytoplasm, a complete cell membrane, and a nucleus. In the kidney tissue, the integrity of the glomerulus was intact. CA<sub>t</sub> extract treatment did not induce any obvious pathological morphology. Taken together, CA<sub>t</sub> extract had little toxicity towards organs, and these data confirm the *in vitro* cytotoxicity evaluation, suggesting that CA<sub>t</sub> extract might have few side effects in a human clinical trial.

Taken together, the results show that CA<sub>t</sub> extract had an inhibitory effect on HCC tumor cell growth through the induction of apoptosis, the arrest of the cell cycle, the repression of autocrine signaling, and the inhibition of AKT/ERK/p38 signaling. Moreover, CA<sub>t</sub> extract has a potential capacity for the suppression of invasion. The evaluation of toxicity in the xenograft model revealed no or few changes in the mice. As a result, our findings provide a basis for further studies of CA<sub>t</sub> extract in the treatment of HCC. However, additional investigation is needed to clarify the molecular pathway precisely. Overall, it can be said that CA<sub>t</sub> extract has the potential for clinical applications *in vitro* and *in vivo* against HCC.

## 4. Materials and Methods

### 4.1. Cell Culture

Human hepatocellular carcinoma cells (HepG<sub>2</sub>, Mahlavu, Huh7 and J5), mouse normal liver embryonic cells (BNL CL.2), mouse normal endothelial cells (SVEC), and canine normal kidney epithelial cells (MDCK) were purchased from the American Type Culture Collection (Manassas, VA, USA) and the Bioresource Collection and Research Center (Hsinchu, Taiwan). The cells were grown in Dulbecco's modified Eagle's medium (HepG<sub>2</sub>, Mahlavu, Huh7, BNL CL.2, SVEC, and MDCK cells) or Roswell Park Memorial Institute 1640 (J5 cell) supplemented with 10% fetal bovine serum, 1% sodium pyruvate, 1% HEPES, and 1% penicillin/streptomycin in an incubator containing 5% CO<sub>2</sub> at 37 °C. All reagents were purchased from Gibco (Waltham, MA, USA). The status of the genes in the cells was determined by the FemtoPath Primer Set (HongJing Biotech, New Taipei City, Taiwan).

### 4.2. Extraction of *Cedrus atlantica* Plant Material

The steam-distilled preparation of *Cedrus atlantica* extract (CA<sub>t</sub> extract) was purchased from PHOENIX (Red Bank, NJ, USA). For small-scale extraction, fresh bark of a *Cedrus atlantica* plant (500 g) was used, which was originally from America. The flow rate of generated steam was 7.2 mL/min, passed through the plant material at 100~105 °C for 100 min. After extraction, two layers were formed: one was the aqueous layer, and the other was the lipid layer utilized throughout the experiments. The extracted CA<sub>t</sub> solution (lipid layer) was aliquoted and sealed in a brown glass bottle and then stored at 4 °C. The CA<sub>t</sub> extract concentration was calculated in µg/mL and was diluted in DMSO (Sigma Aldrich, Saint Louis, MI, USA) such that the final concentration of solvent in culture media did not exceed 0.2%.

### 4.3. Cytotoxicity of the CA<sub>t</sub> Extract on HCC Cells

HCC cells ( $5 \times 10^3$  cells/well), BNL CL.2 ( $4 \times 10^4$  cells/well), MDCK, and SVEC ( $1 \times 10^4$  cells/well) were seeded and grown in 96-well plates overnight. Cells were treated with vehicle (0.1% DMSO) and serial concentrations of the CA<sub>t</sub> extract (0–200 µg/mL) for 24, 48, and 72 h. Cell viability was measured by MTT-based colorimetric assays. The formazan crystals formed were solubilized by DMSO, and the absorbance was measured at a wavelength of 550 nm by a SpectraMax M5 microplate reader (Molecular

Devices, San Jose, CA, USA). The effective absorbance was calculated for cell viability (%), which was presented as treatment (OD)/vehicle (OD)  $\times$  100%. The experiments were analyzed in triplicate.

#### 4.4. Flow Cytometric Analysis

HepG<sub>2</sub> and Mahlavu cells were plated in 10 cm dishes at a density of  $2 \times 10^6$ , incubated overnight, and treated for 6, 12, 24, or 48 h with the indicated concentration of the CA<sub>t</sub> extract. The cells were trypsinized, washed with PBS, and resuspended in PBS containing 40  $\mu$ g/mL propidium iodide (PI, Sigma Aldrich, Saint Louis, MO, USA) and 100  $\mu$ g/mL of RNase A (Sigma Aldrich, Saint Louis, MO, USA) overnight in the dark. The cell cycle progression was detected by a FACS Calibur instrument (BD, Franklin Lakes, NJ, USA), and the percentage of cell cycle distribution was analyzed by FlowJo 7.6.1 (Ashland, OR, USA). Values given are the mean  $\pm$  SD of three different experiments performed in triplicate.

#### 4.5. TUNEL Assay

HepG<sub>2</sub> and Mahlavu cells ( $2 \times 10^5$ ) were seeded in 6-well plates overnight. The cells were treated with vehicle or the CA<sub>t</sub> extract (25 or 30  $\mu$ g/mL) for 24 h. The cells were fixed using 4% formaldehyde/methanol at 4 °C for 10 min on slides and stained with terminal deoxynucleotidyl transferase (TdT) according to the manufacturer's instructions (In Situ Cell Death Detection Kit, Roche, Basel, Switzerland). After PI staining (10  $\mu$ g/mL), the slides were sealed with a cover glass. Each experiment was carried out in triplicate. The fluorescence was visualized by microscopy (ZEISS Axio Imager A2, Bremen, Germany) under  $\times$ 400 field and the images were adjusted in Photoshop (Adobe, San Jose, CA, USA).

#### 4.6. Western Blot Analysis

HepG<sub>2</sub> and Mahlavu cells ( $2 \times 10^6$ ) were grown in 10 cm dishes overnight and treated with the CA<sub>t</sub> extract at different time points with the indicated CA<sub>t</sub> extract concentration. The protein concentration was measured by the BCA Protein Assay Reagent (Thermo Fisher Scientific, Waltham, MA, USA), according to the manufacturer's instructions. The proteins were resolved by 8–12% SDS-PAGE and transferred to PVDF membranes. After blocking with skimmed milk, the membranes were incubated with primary antibodies overnight at 4 °C, then incubated with secondary antibodies conjugated to HRP (horseradish peroxidase) for 2 h at room temperature. Enhanced chemiluminescence detection reagents (T-Pro Biotechnology, New Taipei City, Taiwan) were used to visualize the protein expression, and the images were analyzed by a LAS-4000 Luminescence/Fluorescence Imaging System (GE Healthcare, Uppsala, Sweden). The protein expression was quantified using ImageJ software (NIH, Bethesda, MD, USA). All of the primary and secondary antibodies were purchased from Santa Cruz Biotechnology, Inc. (Dallas, TX, USA) and iReal Biotechnology Co., Ltd. (Hsinchu, Taiwan). All analyses were performed in biological duplicates.

#### 4.7. HCC Xenograft Model

Female BALB/c nude mice (6–8 weeks old) were obtained from the National Laboratory Animal Center, Taipei, Taiwan. All animal work was conducted in accordance with the protocol approved by the Laboratory Animal Center of Chung Shan Medical University (Taichung, Taiwan; no. CSMU-IACUC-1662). HepG<sub>2</sub> cells ( $1 \times 10^6$ /100  $\mu$ L/mouse) were subcutaneously injected into the right-backs of the mice, and drug administration was initiated five days later. All mice with xenografts were randomly separated into two groups: one was vehicle-treated with mineral oil, 100  $\mu$ L ( $n = 6$ ), and the other was treated with 200 mg/kg/100  $\mu$ L CA<sub>t</sub> extract ( $n = 10$ ). Treatments were given every two days by subcutaneous injection and, meanwhile, the tumor volume and the body weight were recorded. The tumor volume (TV) was calculated using the formula: length  $\times$  width  $\times$  height. All of the mice were sacrificed when the tumor volume reached 2000 mm<sup>3</sup> as the last survival day. After sacrifice, the tumors and organs (heart, liver, spleen, lung, kidney, stomach, and intestine) were collected.

The tissues were fixed with 10% neutral formalin and embedded in paraffin for immunohistochemical and H&E staining. The photographs were taken at  $\times 400$  by microscopy (ZEISS Axio Imager A2, Bremen, Germany).

#### 4.8. Immunohistochemistry (IHC) and Hematoxylin/Eosin (H&E) Staining

Excised tumors and organs were fixed in 10% formalin and embedded in paraffin wax. The tissues were stained with hematoxylin/eosin and examined under  $\times 200$  light microscope to assess the morphological changes. Apoptotic cells in tumor tissues were detected by In Situ Cell Death Detection Kit (Roche, Basel, Switzerland), performed according to the manufacturer's instructions, and the photographs were observed under  $\times 400$  fluorescent microscope. Cleaved caspase-3, PCNA, VEGF, VEGFR1, VEGFR2, MMP2, and MMP9 were stained by the immunohistochemical procedure to observe the indicated protein expressions under  $\times 400$  light microscope. All of the primary and secondary antibodies were purchased from Santa Cruz Biotechnology, Inc. (Dallas, TX, USA).

#### 4.9. Gas Chromatography-Mass Spectrometry (GC-MS) Analysis of CA1 Extract

GC-MS analysis was commissioned to the National Central Taiwan University Office of Research and Development's Center for Advanced Instrumentation (Hsinchu, Taiwan). The sample was diluted using hexane (1/500), the carrier gas was helium (1 mL/min), and the injector temperature was 300 °C with an injection flow rate of 1 mL/min. Agilent 7890CB gas chromatograph (AccuTOF-GCx, Jeol, MA, USA) with an Rxi-5MS capillary column (film thickness: 30 m  $\times$  0.25 mm  $\times$  0.25  $\mu$ m) was utilized to conduct GC-MS. Components were identified by comparing their mass spectra with those obtained from authentic samples or spectra of the Wiley/NIST libraries.

#### 4.10. Statistical Calculations

Results are expressed as means  $\pm$  SD. Differences between groups were compared by Student's *t*-test. Differences within groups were analyzed with the repeated measures two-way Kaplan–Meier estimator, and  $p < 0.05$  was considered statistically significant.

**Author Contributions:** Conceptualization, N.-M.T.; methodology, X.-F.H. and K.-F.C.; software, X.-F.H., S.-C.L., and K.-F.C.; validation, X.-F.H., S.-C.L., and K.-F.C.; formal analysis, X.-F.H. and K.-F.C.; investigation, X.-F.H. and K.-F.C.; resources, C.-Y.H., C.-Y.L., and J.-C.W.; data curation, X.-F.H., K.-F.C., and N.-M.T.; writing—original draft preparation, X.-F.H., C.-Y.H., and N.-M.T.; writing—review and editing, X.-F.H., G.-T.S., C.-Y.H., and N.-M.T.; visualization, N.-M.T.; supervision, N.-M.T.; project administration, N.-M.T.; funding acquisition, C.-Y.H. and N.-M.T. All authors have read and agreed to the published version of the manuscript.

**Funding:** The work was supported by the research grant MOST 105-2320-B-040-025 and MOST 109-2320-B-040-012 from the Ministry of Science and Technology, Taiwan.

**Acknowledgments:** ZEISS Axio Imager A2 microscopy was performed in the Instrument Center of Chung Shan Medical University, which is supported by the National Science Council, the Ministry of Education, and Chung Shan Medical University.

**Conflicts of Interest:** There are no conflicts of interest.

## References

1. Bray, F.; Me, J.F.; Soerjomataram, I.; Siegel, R.; Torre, L.A.; Jemal, A. Global cancer statistics 2018: GLOBOCAN estimates of incidence and mortality worldwide for 36 cancers in 185 countries. *CA Cancer J. Clin.* **2018**, *68*, 394–424. [[CrossRef](#)] [[PubMed](#)]
2. Ikeda, M.; Morizane, C.; Ueno, M.; Okusaka, T.; Ishii, H.; Furuse, J. Chemotherapy for hepatocellular carcinoma: Current status and future perspectives. *Jpn. J. Clin. Oncol.* **2017**, *48*, 103–114. [[CrossRef](#)] [[PubMed](#)]
3. Raoul, J.L.; Forner, A.; Bolondi, L.; Cheung, T.T.; Kloeckner, R.; De Baere, T. Updated use of TACE for hepatocellular carcinoma treatment: How and when to use it based on clinical evidence. *Cancer Treat. Rev.* **2019**, *72*, 28–36. [[CrossRef](#)] [[PubMed](#)]

4. Kudo, M. Systemic Therapy for Hepatocellular Carcinoma: 2017 Update. *Oncology* **2017**, *93*, 135–146. [[CrossRef](#)] [[PubMed](#)]
5. Mak, L.; Cruz-Ramón, V.; Chinchilla-López, P.; Torres, H.A.; LoConte, N.K.; Rice, J.P.; Foxhall, L.E.; Sturgis, E.M.; Merrill, J.K.; Bailey, H.H.; et al. Global Epidemiology, Prevention, and Management of Hepatocellular Carcinoma. *Am. Soc. Clin. Oncol. Educ. Book* **2018**, *38*, 262–279. [[CrossRef](#)]
6. Etik, D.O.; Suna, N.; Boyacioglu, S. Management of Hepatocellular Carcinoma: Prevention, Surveillance, Diagnosis, and Staging. *Exp. Clin. Transplant.* **2017**, *15*, 31–35. [[CrossRef](#)]
7. Kinghorn, A.D.; Farnsworth, N.; Soejarto, D.; Cordell, G.; Swanson, S.; Pezzuto, J.; Wani, M.; Wall, M.; Oberlies, N.H.; Kroll, D.; et al. Novel Strategies for the Discovery of Plant-Derived Anticancer Agents. *Pharm. Biol.* **2003**, *41*, 53–67. [[CrossRef](#)]
8. Dai, J.; Mumper, R.J. Plant Phenolics: Extraction, Analysis and Their Antioxidant and Anticancer Properties. *Molecules* **2010**, *15*, 7313–7352. [[CrossRef](#)]
9. Fitsiou, E.; Pappa, A. Anticancer Activity of Essential Oils and Other Extracts from Aromatic Plants Grown in Greece. *Antioxidants* **2019**, *8*, 290. [[CrossRef](#)]
10. Lin, S.-R.; Chang, C.; Hsu, C.; Tsai, M.; Cheng, H.; Leong, M.K.; Sung, P.; Chen, J.; Weng, C.-F. Natural compounds as potential adjuvants to cancer therapy: Preclinical evidence. *Br. J. Pharmacol.* **2019**, *177*, 1409–1423. [[CrossRef](#)]
11. Shinde, U.; Phadke, A.; Nair, A.; Mungantiwar, A.; Dikshit, V.; Saraf, M. Studies on the anti-inflammatory and analgesic activity of Cedrus deodara (Roxb.) Loud. wood oil. *J. Ethnopharmacol.* **1999**, *65*, 21–27. [[CrossRef](#)]
12. Sharma, P.R.; Shanmugavel, M.; Saxena, A.K.; Qazi, G.N. Induction of apoptosis by a synergistic lignan composition from Cedrus deodara in human cancer cells. *Phytotherapy Res.* **2008**, *22*, 1587–1594. [[CrossRef](#)] [[PubMed](#)]
13. Shashi, B.; Jaswant, S.; Madhusudana, R.J.; Kumar, S.A.; Nabi, Q.G. A novel lignan composition from Cedrus deodara induces apoptosis and early nitric oxide generation in human leukemia Molt-4 and HL-60 cells. *Nitric. Oxide* **2006**, *14*, 72–88. [[CrossRef](#)] [[PubMed](#)]
14. Shid, X.; Liu, N.; Zhang, J.; Hu, P.; Shen, W.; Fan, B.; Ma, Q.; Wang, X. Extraction and purification of total flavonoids from pine needles of Cedrus deodara contribute to anti-tumor in vitro. *BMC Complement. Altern. Med.* **2016**, *16*, 245. [[CrossRef](#)]
15. Singh, S.; Shanmugavel, M.; Kampasi, H.; Singh, R.; Mondhe, D.; Rao, J.; Adwankar, M.; Saxena, A.; Qazi, G. Chemically Standardized Isolates from Cedrus deodara Stem Wood having Anticancer Activity. *Planta Med.* **2007**, *73*, 519–526. [[CrossRef](#)]
16. Saxena, A.; Saxena, A.K.; Singh, J.; Bhushan, S. Natural antioxidants synergistically enhance the anticancer potential of AP9-cd, a novel lignan composition from Cedrus deodara in human leukemia HL-60 cells. *Chem. Biol. Interact.* **2010**, *188*, 580–590. [[CrossRef](#)]
17. Tiwari, A.K.; Srinivas, P.V.; Kumar, S.P.; Rao, J.M. Free radical scavenging active components from Cedrus deodara. *J. Agric. Food Chem.* **2001**, *49*, 4642–4645. [[CrossRef](#)]
18. Chaudhary, A.; Sood, S.; Kaur, P.; Kumar, N.; Thakur, A.; Gulati, A.; Singh, B. Antifungal Sesquiterpenes from Cedrus deodara. *Planta Med.* **2011**, *78*, 186–188. [[CrossRef](#)]
19. Uehara, A.; Tommis, B.; Belhassen, E.; Satrani, B.; Ghanmi, M.; Baldovini, N. Odor-active constituents of Cedrus atlantica wood essential oil. *Phytochemistry* **2017**, *144*, 208–215. [[CrossRef](#)]
20. Dakir, M.; El Hanbali, F.; Mellouki, F.; Akssira, M.; Benharref, A.; Del Moral, J.F.Q.; Barrero, A.F.; Del Moral, J.F.Q. Antibacterial diterpenoids from Cedrus atlantica. *Nat. Prod. Res.* **2005**, *19*, 719–722. [[CrossRef](#)]
21. Martins, D.F.; Emer, A.A.; Batisti, A.; Donatello, N.; Carlesso, M.G.; Martins, D.F.; Venzke, D.; Micke, G.A.; Pizzolatti, M.G.; Piovezan, A.; et al. Inhalation of Cedrus atlantica essential oil alleviates pain behavior through activation of descending pain modulation pathways in a mouse model of postoperative pain. *J. Ethnopharmacol.* **2015**, *175*, 30–38. [[CrossRef](#)] [[PubMed](#)]
22. Brigitte Bressac, K.M.G.; Liang, T.J.; Isselbacher, K.J.; Wands, J.R.; Ozturk, M. Abnormal structure and expression of p53 gene in human hepatocellular carcinoma. *Proc. Natl. Acad. Sci. USA* **1990**, *87*, 1973–1977. [[CrossRef](#)] [[PubMed](#)]
23. Chen, C.-Y.; Liu, T.-Z.; Liu, Y.; Tseng, W.-C.; Liu, R.H.; Lu, F.-J.; Lin, Y.-S.; Kuo, S.-H.; Chen, C.-H. 6-Shogaol (Alkanone from Ginger) Induces Apoptotic Cell Death of Human Hepatoma p53 Mutant Mahlavu Subline

- via an Oxidative Stress-Mediated Caspase-Dependent Mechanism. *J. Agric. Food Chem.* **2007**, *55*, 948–954. [[CrossRef](#)] [[PubMed](#)]
24. Liu, Li, W.; Tan, N.; Zhang, Z.; Liang, J.J.; Brown, R.E. Activation of Akt-mTOR-p70S6K pathway in angiogenesis in hepatocellular carcinoma. *Oncol. Rep.* **2008**, *20*, 713–719. [[CrossRef](#)]
  25. Yang, S.; Liu, G. Targeting the Ras/Raf/MEK/ERK pathway in hepatocellular carcinoma. *Oncol. Lett.* **2017**, *13*, 1041–1047. [[CrossRef](#)]
  26. Zhang, S.-Y.; Li, X.-B.; Hou, S.-G.; Sun, Y.; Shi, Y.-R.; Lin, S.-S. Cedrol induces autophagy and apoptotic cell death in A549 non-small cell lung carcinoma cells through the P13K/Akt signaling pathway, the loss of mitochondrial transmembrane potential and the generation of ROS. *Int. J. Mol. Med.* **2016**, *38*, 291–299. [[CrossRef](#)]
  27. Zhan, P.; Ji, Y.-N.; Yu, L.-K. TP53 mutation is associated with a poor outcome for patients with hepatocellular carcinoma: Evidence from a meta-analysis. *HepatoBiliary Surg. Nutr.* **2013**, *2*, 260–265.
  28. Wysocki, P.J. Targeted therapy of hepatocellular cancer. *Expert Opin. Investig. Drugs* **2010**, *19*, 265–274. [[CrossRef](#)]
  29. Matter, M.; Decaens, T.; Andersen, J.B.; Thorgeirsson, S.S. Targeting the mTOR pathway in hepatocellular carcinoma: Current state and future trends. *J. Hepatol.* **2013**, *60*, 855–865. [[CrossRef](#)]
  30. Kunter, I.; Erdal, E.; Nart, D.; Yilmaz, F.; Karademir, S.; Sagol, O.; Atabey, N. Active form of AKT controls cell proliferation and response to apoptosis in hepatocellular carcinoma. *Oncol. Rep.* **2013**, *31*, 573–580. [[CrossRef](#)]
  31. Huynh, H. Molecularly targeted therapy in hepatocellular carcinoma. *Biochem. Pharmacol.* **2010**, *80*, 550–560. [[CrossRef](#)] [[PubMed](#)]
  32. Strzalka, W.; Ziemienowicz, A. Proliferating cell nuclear antigen (PCNA): A key factor in DNA replication and cell cycle regulation. *Ann. Bot.* **2010**, *107*, 1127–1140. [[CrossRef](#)] [[PubMed](#)]
  33. Masood, R.; Cai, J.; Zheng, T.; Smith, D.; Hinton, D.R.; Gill, P.S. Vascular endothelial growth factor (VEGF) is an autocrine growth factor for VEGF receptor-positive human tumors. *Blood* **2001**, *98*, 1904–1913. [[CrossRef](#)] [[PubMed](#)]
  34. Sporn, M.B.; Roberts, A.B. Autocrine growth factors and cancer. *Nat. Cell Biol.* **1985**, *313*, 745–747. [[CrossRef](#)] [[PubMed](#)]
  35. Muto, J.; Shirabe, K.; Sugimachi, K.; Maehara, Y. Review of angiogenesis in hepatocellular carcinoma. *Hepatol. Res.* **2014**, *45*, 1–9. [[CrossRef](#)]
  36. Finn, R.S.; Zhu, A.X. Targeting angiogenesis in hepatocellular carcinoma: Focus on VEGF and bevacizumab. *Expert Rev. Anticancer. Ther.* **2009**, *9*, 503–509. [[CrossRef](#)]
  37. He, Y.-H.; Li, M.-F.; Zhang, X.-Y.; Meng, X.-M.; Huang, C.; Li, J. NLRC5 promotes cell proliferation via regulating the AKT/VEGF-A signaling pathway in hepatocellular carcinoma. *Toxicology* **2016**, *47*–57. [[CrossRef](#)]
  38. Hoshida, Y.; Toffanin, S.; Lachenmayer, A.; Villanueva, A.; Minguez, B.; Llovet, J.M. Molecular Classification and Novel Targets in Hepatocellular Carcinoma: Recent Advancements. *Semin. Liver Dis.* **2010**, *30*, 035–051. [[CrossRef](#)]
  39. Zhang, G.; Li, Z.; Wan, X.; Zhang, Y.; Zhu, R.; Liu, Z.; Ji, D.; Zhang, H.; Wu, F.; Tian, H.; et al. Repression of Human Hepatocellular Carcinoma Growth by Regulating Met/EGFR/VEGFR-Akt/NF- $\kappa$ B Pathways with Theanine and Its Derivative, (R)-2-(6,8-Dibromo-2-oxo-2H-chromene-3-carboxamido)-5-(ethylamino)-5-oxopentanoic Ethyl Ester (DTBrC). *J. Agric. Food Chem.* **2016**, *64*, 7002–7013. [[CrossRef](#)]

**Sample Availability:** Samples of the compounds not available are available from the authors.



© 2020 by the authors. Licensee MDPI, Basel, Switzerland. This article is an open access article distributed under the terms and conditions of the Creative Commons Attribution (CC BY) license (<http://creativecommons.org/licenses/by/4.0/>).